

An electrically-activated dynamic tissue-equivalent phantom for assessment of diffuse optical imaging systems

Jeremy C Hebden, Joanna Brunker, Teresa Correia, Ben D Price,
Adam P Gibson and N L Everdell

Department of Medical Physics & Bioengineering, University College London, Gower Street,
London WC1E 6BT, UK

Received 15 November 2007

Published 28 December 2007

Online at stacks.iop.org/PMB/53/329

Abstract

A novel design of solid dynamic phantom with tissue-like optical properties is presented, which contains variable regions of contrast which are activated electrically. Reversible changes in absorption are produced by localized heating of targets impregnated with thermochromic pigment. A portable, battery-operated prototype has been constructed, and its optical and temporal characteristics have been investigated. The phantom has been developed as a means of assessing the performance of diffuse optical imaging systems, such as those used to monitor haemodynamic changes in the brain and other tissues. Images of the phantom have been reconstructed using data acquired with a continuous wave optical topography system.

1. Introduction

Diffuse optical imaging has become a popular research tool for studying blood flow and oxygenation in biological tissues, and in the brain in particular (Franceschini and Boas 2004, Gibson *et al* 2005, Gratton *et al* 2005). The technique involves illuminating the tissue with near-infrared light, and measuring that which has been diffusely transmitted, as a result of multiple scattering, through the regions of interest. Significant difference between the characteristic absorptions of the oxygenated and de-oxygenated forms of haemoglobin at near-infrared wavelengths enables haemodynamics and blood oxygenation to be monitored non-invasively. While the generation of three-dimensional (3D) images representing absolute values of tissue properties is regarded as highly desirable, this represents a technically challenging task and requires a significant theoretical formulation to tackle the ill-posed and ill-conditioned reconstruction problem (Arridge 1999). A much simpler and more common approach to diffuse optical imaging is to generate images of changes in optical properties which occur due to a natural or induced alteration in blood volume and/or oxygenation. This requires obtaining two sets of data, before and after the change, which can normally be achieved in

rapid succession without adjustments to the instrument. So-called difference imaging has been shown to be highly robust to various simplifying assumptions and allows a straightforward 'linear' reconstruction to be applied (Gibson *et al* 2003).

Two closely-related diffuse optical imaging approaches have been developed, known as optical tomography and optical topography. Although the distinction between them is somewhat arbitrary, optical tomography is usually used to describe techniques which acquire images representing the 3D volume of tissue or a transverse slice, while optical topography involves providing maps of changes in optical properties (usually absorption) close to the surface, with little or no depth resolution. For optical topography, measurements of diffusely reflected light are acquired at small (<3 cm) source-detector separations over a selected area of tissue. Optical topography has been widely used to study the evoked response of the brain to a broad variety of sensory stimuli (Blasi *et al* 2007, Franceschini *et al* 2003, Kotilahti *et al* 2005, Taga *et al* 2003, Zeff *et al* 2007). The relatively small separations ensure that measured signals are relatively high and therefore may be acquired quickly, enabling brain activity with characteristic responses as fast as a 100 ms or so to be studied, and images to be displayed in real-time. However, the small separations restrict the sensitivity to surface (cortical) tissues.

Like that of any other medical diagnostic modality, the development of optical imaging techniques relies upon appropriate phantoms with tissue-like properties to evaluate the system performance and to validate imaging algorithms (Pogue and Patterson 2006). The assessment of imaging systems designed to display haemodynamic and functional changes benefits in particular from phantoms which can provide controlled, localized changes in optical properties. Several basic designs of dynamic phantom have been described in the published literature. One approach involves physically moving (with the aid of an electric motor) a target of contrasting optical properties within an otherwise uniform absorbing and scattering liquid (Yamashita *et al* 1999, Schmitz *et al* 2002, Everdell *et al* 2005). This facilitates rapid periodic variation which is useful for characterizing temporal, spatial and contrast resolution. To assess the quantitative accuracy of optical techniques, some investigators have developed liquid phantoms containing static or flowing blood, whose oxygenation state can be varied and independently determined (Kurth *et al* 1995, Wolf *et al* 1999, Li *et al* 2004).

In general, solid phantoms offer significant advantages over those based on liquids: they do not require a containing vessel, they are more easily stored and transported, and they are often more stable over time. A solid dynamic phantom designed to study the effects of laser irradiation has been developed by Iizuka *et al* (1999). This is based on a polysaccharide gel (agar) containing albumen (egg white), which undergoes an irreversible increase in optical scatter when heated as a result of thermal coagulation. The first solid dynamic phantom containing a reversible, electrically-activated region has been developed by NIRx Medical Technologies (USA). This is based on electrochromic materials embedded in a solid plastic with realistic tissue geometry (Barbour *et al* 2006). The optical opacity of the material can be modulated with millisecond response times to mimic the temporal and wavelength changes associated with haemodynamic activity.

In this paper, we present an alternative design of solid dynamic phantom, based on thermochromic dye. A thermochromic substance is able to change colour (i.e. change its optical absorption characteristics) in response to a change in temperature. The reversible change typically occurs over a temperature range of a few degrees, centred on the so-called activation temperature. Industrial thermochromic dyes are available with a broad range of activation temperatures, and which change between a range of colours. In principle, the dyes can be mixed with various plastics and other substances to produce media with tissue-like optical properties, and changes in absorption are introduced by heating above (or cooling below) the activation temperature. The dye can be localized within specific regions or

distributed globally, and heating can be localized internally or applied externally. The design of a battery-operated prototype phantom is described in the following section, followed by an assessment of its optical and temporal characteristics and a report on the result of an optical imaging experiment.

2. Phantom design

A thermochromic dye was obtained in the form of a black ChromaZone[®] powder (Thermographic Measurements Co. Ltd, UK). ChromaZone[®] powder consists of individual droplets of thermochromic pigment encapsulated in an impervious polymeric shell. The particle shell is designed to withstand most standard mixing and application procedures, and the mean particle size is around 4 μm . Each particle contains a colorant and an organic acid suspended within a low melting point solvent. In the solid state, interactions between electrons in the colorant and organic acid produce an optical absorption band which gives the powder its characteristic colour. In the liquid state, the components can separate, and the absorption no longer occurs. When heated, the black ChromaZone[®] powder changes from black to white over a temperature range of about 5 $^{\circ}\text{C}$, with a nominal activation temperature of 47 $^{\circ}\text{C}$. The change is also characterized by a thermal hysteresis: the reverse colour change on cooling occurs over an equivalent range but at a temperature which is several degrees cooler. Users of ChromaZone[®] are notified that the thermochromic properties can be disrupted by various external influences such as exposure to excessive temperatures, to ultraviolet light, and to polar solvents and other aggressive chemicals. The powder stored in a cool, dark environment is guaranteed a shelf life of 12 months.

To produce a material suitable for generating a solid tissue-equivalent phantom, we mixed the powder with either a two-component epoxy resin (MY753, Aeropia Chemical Supplies, UK) or a polyester resin (Alec Tiranti Ltd, UK). Neither resin appeared to produce a direct chemical effect on the thermochromic properties. However, heat generated exothermically during setting of the epoxy resin destroyed the thermochromic properties unless the volume of resin was small ($< \text{few cm}^3$) or the resin was refrigerated during the setting process. The attenuating properties of the pigment were examined using thin (~ 6 mm) samples of solid resin containing known concentrations of pigment. A collimated source and detector were used to estimate the specific attenuation coefficient of the pigment at room temperature and at 50 $^{\circ}\text{C}$ at selected wavelengths. Curiously, while heating of the pigment clearly exhibited a decrease in specific attenuation coefficient at visible wavelengths, heating produced a slight increase in the coefficient at higher (> 800 nm) wavelengths. Furthermore, a visual inspection of the samples indicated that while scatter was a negligible contributor to the attenuation at room temperature, the change in colour from black to white on heating was accompanied by a moderate increase in turbidity.

Two target objects to be inserted within the phantom were generated by mixing powder with the polyester resin in a small plastic cylindrical tube. Targets A and B correspond to powder concentrations of 16 mg cm^{-3} and 6.5 mg cm^{-3} , respectively. Before setting, a small 11 Ω surface mount resistor was placed inside the resin/powder mixture, together with a pre-calibrated 4.7 k Ω bead thermistor, as illustrated in figure 1(a). When extracted from the tube, each target was a 8 mm diameter cylinder with a height of 8 mm. Meanwhile, a block of polyester resin mixed with titanium dioxide particles was produced with a transport scattering coefficient $\mu'_s = 1.0 \pm 0.1 \text{ mm}^{-1}$ and an absorption coefficient $\mu_a = 0.001 \pm 0.0002 \text{ mm}^{-1}$ over the 650–850 nm wavelength range (Firbank and Delpy 1993). The dimensions of the block were 130 mm \times 130 mm \times 35 mm. The two targets were embedded inside the block at a depth of 10 mm below the top surface, 30 mm apart as shown in figure 1(b). The thin

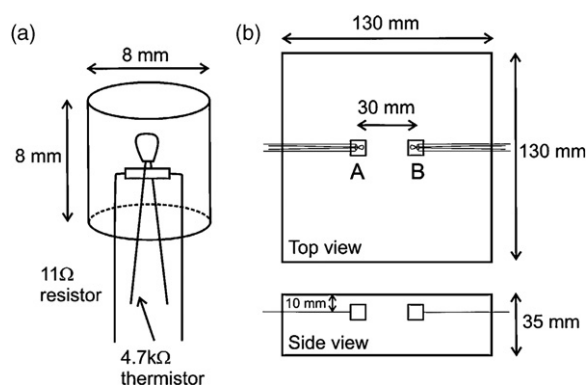


Figure 1. (a) A resin target containing thermochromic dye in which a heating resistor and thermistor are embedded; (b) a schematic of the slab phantom containing two electrically-activated targets A and B with different concentrations of thermochromic dye.

(400 μm) wires connected to each heating resistor and thermistor exit the phantom at opposite sides.

In the final phantom, operating a switch connects either resistor to three 1.2 V rechargeable cells in series, providing a heating power of about 1.2 W. If all the heat were confined to the target and uniformly distributed within it, a calculation based on the thermal properties of polyester resin (Kosar *et al* 2005) indicates that the temperature of the target would rise at a rate of approximately $1.5\text{ }^{\circ}\text{C s}^{-1}$. Thus the entire target starting at room temperature would exceed the activation temperature after about 20 s. In practice, diffusion of heat to the surrounding resin reduces the rate of temperature increase. Tests using identical targets embedded in similar volumes of clear resin demonstrated that the targets undergo a colour change within about 50 s. The temperature of either target is monitored by measuring the resistance of the embedded thermistors. To avoid damage due to excess heating, the switch is opened a few seconds after the thermistor indicates that the activation temperature is reached.

3. Phantom measurements

3.1. Transmission measurements

Prior to optical imaging of the phantom, transmission measurements were made across the 35 mm thickness to confirm the change in attenuation produced by the target with the highest concentration of thermochromic pigment (A) as a function of wavelength, time and temperature. Optical fibres connected to a broadband source and a spectrometer were coupled to either side of the phantom in line with target A. Spectra were then recorded continuously as the target was heated from room temperature until the thermistor gave a reading of $50\text{ }^{\circ}\text{C}$, and then while the phantom was allowed to cool.

The spectra obtained at the two extreme temperatures were used to calculate the change in transmittance as a function of wavelength produced by the thermochromic reaction within target A. This change is illustrated in figure 2 in units of optical densities, equal to the log base 10 of the intensity ratios. As expected, at lower (visible) wavelengths, the transmittance increases as the target changes colour from black to white. The figure also confirms a transmittance change in the opposite direction at near-infrared wavelengths above 790 nm.

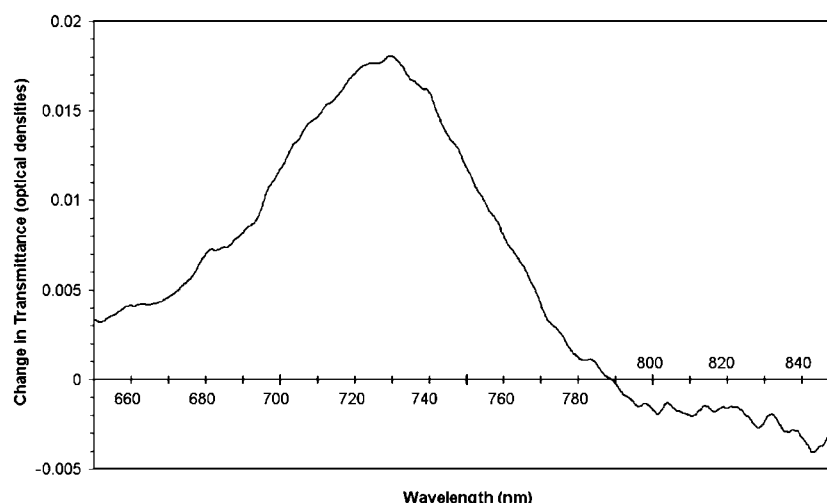


Figure 2. The change in optical density as a function of wavelength measured across the phantom in line with target A when the target was heated from room temperature to above the activation temperature.

However, it has not been determined whether this decrease in transmittance is primarily due to an increase in absorption or an increase in scatter (as observed at visible wavelengths).

The temporal characteristics of the phantom are illustrated in figure 3 for a wavelength of 690 nm. The switch is closed at time zero on the horizontal axis, and opened after 50 s when the temperature reaches 50 °C. Each measurement of transmitted intensity at 690 nm was integrated over 5 s. The figure shows that about 10 s elapses before any part of the target reaches the activation temperature, and thereafter the intensity increases roughly linearly with time until the switch is opened. The first measurement taken 5 s after the electrical heating is terminated shows that regions of the target have continued to rise above the activation temperature. The transmitted intensity then falls rapidly as the heat diffuses away from the target. The target has apparently regained most of its black colour after about 30 s, but requires a further minute or so to completely return to its initial state.

The asymmetry exhibited in figure 3 is partly dependent on the thermal hysteresis of the thermochromic pigment. This hysteresis is exhibited in figure 4, which shows the change in transmitted intensity measured across the phantom at a wavelength of 690 nm as a function of thermistor temperature when the target A was heated (solid circles) and then allowed to cool (open circles). The intensity change during cooling occurs over a similar range of temperature to that observed during heating, but several degrees cooler. However, it is important to note that the temperature distribution will not be uniform within the target, and therefore regions of the target can be either hotter or cooler than that indicated by the thermistor. The distributions are likely to be different during heating and cooling, even for an identical thermistor temperature.

3.2. Optical imaging

An image of the change in absorption occurring within the phantom was obtained using the UCL optical topography system described by Everdell *et al* (2005). Although the system can support up to 16 detectors and 32 sources at two wavelengths, the phantom measurement

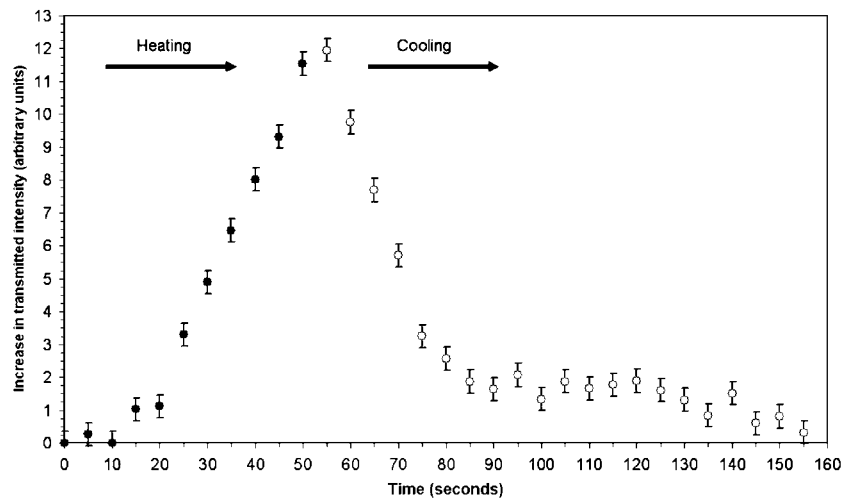


Figure 3. The change in transmitted intensity at a wavelength of 690 nm as a function of time measured across the phantom in line with target A when the target was heated from room temperature to above the activation temperature ● and then allowed to cool ○.

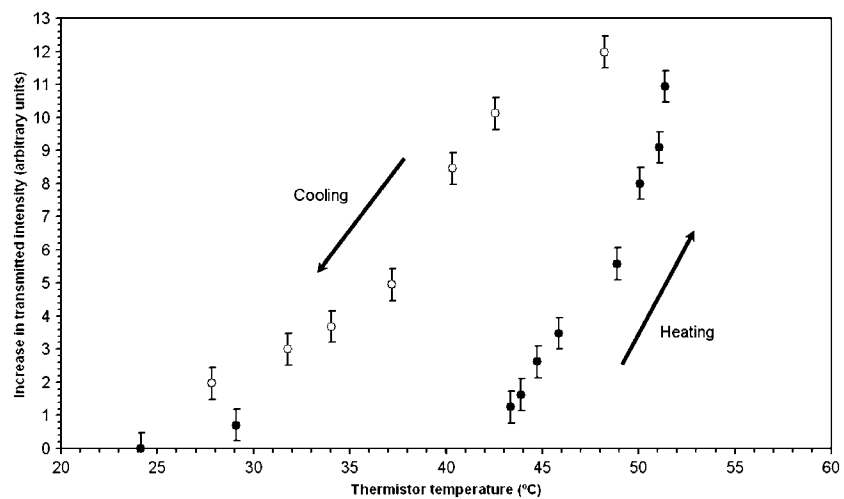


Figure 4. The change in transmitted intensity at a wavelength of 690 nm as a function of thermistor temperature measured across the phantom in line with target A when the target was heated from room temperature to above the activation temperature ● and then allowed to cool ○.

employed a simple square array consisting of just eight detectors and eight sources at a wavelength of 690 nm (each arranged in two rows of four). The array was originally developed to study evoked haemodynamic activity in the brains of infants, and is described in detail in Blasi *et al* (2007). The imaging system illuminates all sources simultaneously, each modulated at a different frequency, and measurements of diffuse reflected intensity are acquired by each detector. A Fourier transform of each detected signal enables the contribution from each source to be isolated at a sampling rate of 10 Hz.

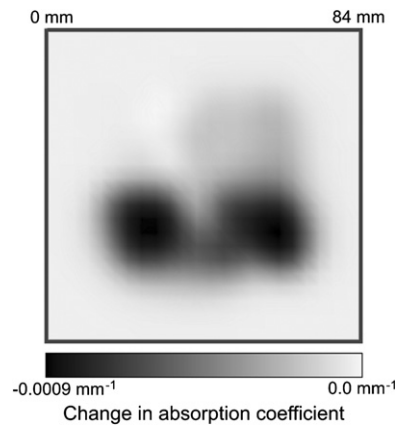


Figure 5. An optical topography image of the phantom reconstructed using differences in diffuse reflected intensity at a wavelength of 690 nm. Target A is on the left and target B is on the right.

The array was placed on the top surface of the phantom, directly above the two targets, and data were acquired continuously for a period of 2 min. Switches were closed to initiate heating of both targets 20 s after the start of the acquisition, and then re-opened when both thermistors indicated a temperature of 50 °C, about 50 s later. The mean signals acquired by each source-detector combination over the first 20 s of data were calculated and stored. A second set of measurements was then computed by averaging signals recorded over a continuous 20 s segment of data centred on the time at which the maximum temperature was reached. The two sets of measurements were then used to reconstruct a three-dimensional (3D) image representing the change in absorption occurring within the phantom directly below the array. A linear image reconstruction algorithm was used, based on the Rytov approximation (Arridge 1999). Internal changes in the optical absorption, Δx , are computed from the differences between the log amplitudes of the two sets of data, Δy , using the matrix equation $\Delta y = J\Delta x$, where J is the Jacobian or sensitivity matrix. The Jacobian was calculated using the TOAST software package (Arridge *et al* 2000) by solving the diffusion equation for a finite element representation of the phantom/array geometry, assuming uniform optical properties ($\mu'_s = 1.0 \text{ mm}^{-1}$ and $\mu_a = 0.001 \text{ mm}^{-1}$). An image representing the 3D distribution of the change in absorption is generated by inverting J . This is achieved using Tikhonov regularization of the Moore–Penrose generalized inverse $\Delta x = J^T (JJ^T + \lambda I)^{-1} \Delta y$, where the regularization parameter λ was set to 0.1% of the largest singular value of JJ^T , and I is the identity matrix.

The image displayed in figure 5 corresponds to a slice across the 3D image at a depth 10 mm below the surface. As expected, the image displays two discrete regions of decreased absorption produced by the two targets. The apparent separation of the targets is about 33 mm, slightly higher than the true centre-to-centre separation of 30 mm. This small discrepancy may be due to the uneven distribution of the colour change within the targets, or due to the localization inaccuracy inherent in the reconstruction algorithm. Target A is on the left and target B on the right. Earlier measurements of the specific attenuation coefficient of the pigment at 690 nm above and below the activation temperature suggest that the actual changes in linear attenuation coefficient of the targets A and B are approximately 0.64 mm^{-1} and 0.26 mm^{-1} , respectively. Assuming attenuation changes at 690 nm are dominated by absorption changes implies that the reconstruction has significantly underestimated the true

change. However, linear methods are inherently unreliable when reconstructing large changes, and are also notoriously sensitive to the choice of regularization parameter λ (Gibson *et al* 2005). The use of a Jacobian based on uniform optical properties (whereas in practice the phantom is not homogeneous at either temperature) will also contribute to error in quantitation.

4. Discussion

Diffuse optical imaging systems are becoming an increasingly popular research tool, and for the study of haemodynamic changes in the brain in particular. Such systems benefit from regular testing on well-characterized phantoms, and we present a design of phantom that provides stable, repeatable measurements and requires no advance preparation. The portable, battery-operated prototype is simple and very convenient to use. It has been constructed from inexpensive, readily available materials and is straightforward to build.

The basic design offers considerable flexibility. There are many types of thermochromic pigments available, which change between a broad variety of colours and at different activation temperatures. Since diffuse optical imaging systems typically operate at wavelengths within the range 650–900 nm, pigments which provide significant changes at near-infrared wavelengths are clearly particularly desirable. Although most industrial applications of thermochromic pigments inevitably require visible changes, the availability of pigments which produce significant changes at longer wavelengths is likely to improve as thermochromic dye technology continues to progress.

A potential limitation of the phantom for some uses is the relatively long period of time required to undergo a full change in optical properties in either direction. The timescale for the prototype is clearly significantly slower than the few seconds associated with haemodynamic changes in the brain. It is feasible that with appropriate selection of pigment and control of the heating mechanism, faster changes could be achieved. The use of pigments with lower activation temperatures would enable the transition temperature to be reached more rapidly and with less electrical energy being required. On the other hand, pigments with higher activation temperatures would allow faster changes to be produced since the heat would be dispersed more quickly. Meanwhile, a simple circuit can be used to monitor the thermistor resistance and automatically terminate the heating current when the activation temperature is exceeded. This would enable targets to be maintained at a roughly constant temperature, just above or just below the activation temperature, enabling faster changes between the two.

Finally, we stress the importance of considering the safety issues when heating solids internally. It is imperative to avoid excessive temperatures and very high rates of heating. Overheating of the targets will certainly destroy their thermochromic properties, and could lead to potentially dangerous disintegration of the phantom. Excessive rates of heating can be avoided by using low-power resistors (or appropriate fuses in series) which will quickly burn out if subjected to excess current.

Acknowledgement

This work has been funded by a Wellcome Trust Vacation Scholarship.

References

- Arridge S R 1999 Optical tomography in medical imaging *Inverse Problems* **15** 41–93
- Arridge S R, Hebden J C, Schweiger M, Schmidt F E W, Fry M E, Hillman E M C, Dehghani H and Delpy D T 2000 A method for 3D time-resolved optical tomography *Int. J. Imaging Syst. Technol.* **11** 2–11

- Barbour R L, Graber H L, Xu Y, Pei Y, Ansari R, Levin M B and Farber M 2006 Diffuse optical tissue simulator (DOTS): an experimental calibrating system for functional DOT imaging *Fifth Inter-Institute Workshop on Optical Diagnostic Imaging from Bench to Bedside at the National Institutes of Health (Bethesda, MD, September 25–27, 2006)*
- Blasi A, Fox S, Everdell N, Volein A, Tucker L, Csibra G, Gibson A P, Hebden J C, Johnson M H and Elwell C E 2007 Investigation of depth dependent changes in cerebral haemodynamics during face perception in infants *Phys. Med. Biol.* **52** 6849–64
- Everdell N L, Gibson A P, Tullis I D C, Vaithianathan T, Hebden J C and Delpy D T 2005 A frequency multiplexed near-infrared topography system for imaging functional activation in the brain *Rev. Sci. Instrum.* **76** 093705
- Firbank M and Delpy D T 1993 A design for a stable and reproducible phantom for use in near-infrared imaging and spectroscopy *Phys. Med. Biol.* **38** 847–53
- Franceschini M A and Boas D A 2004 Noninvasive measurement of neuronal activity with NIR optical imaging *Neuroimage* **21** 372–86
- Franceschini M A, Fantini S, Thompson J H, Culver J P and Boas D A 2003 Hemodynamic evoked response of the sensorimotor cortex measured noninvasively with near-infrared optical imaging *Psychophysiology* **40** 548–60
- Gibson A P, Hebden J C and Arridge S R 2005 Recent advances in diffuse optical imaging *Phys. Med. Biol.* **50** R1–43
- Gibson A P, Yusof R M, Dehghani H, Riley J, Everdell N L, Richards R, Hebden J C, Schweiger M, Arridge S R and Delpy D T 2003 Optical tomography of a realistic neonatal head phantom *Appl. Opt.* **42** 3109–16
- Gratton E, Toronov V, Wolf U, Wolf M and Webb A 2005 Measurement of brain activity by near-infrared light *J. Biomed. Opt.* **10** 011008
- Iizuka M N, Vitkin I A, Kolios M C and Sherar M D 2000 The effects of dynamic optical properties during interstitial laser photocoagulation *Phys. Med. Biol.* **45** 1335–57
- Kosar V, Gomzi Z and Antunović S 2005 Cure of polyester resin in a cylindrical mould heated by air *Thermochimica Acta.* **433** 134–41
- Kotilahti K, Nissilä I, Huutilainen M, Mäkelä R, Gavrielides N, Nojonen T, Björkman P, Fellman V and Katila T 2005 Bilateral hemodynamic responses to auditory stimulation in newborn infants *Brain Imaging* **16** 1373–7
- Kurth C D, Liu H, Thayer W S and Chance B 1995 A dynamic phantom brain model for near-infrared spectroscopy *Phys. Med. Biol.* **40** 2079–92
- Li A, Zhang Q, Culver J P, Miller E L and Boas D A 2004 Reconstructing chromosphere concentration images directly by continuous-wave diffuse optical tomography *Opt. Lett.* **29** 256–8
- Pogue B W and Patterson M S 2006 Review of tissue simulating phantoms for optical spectroscopy, imaging, and dosimetry *J. Biomed. Opt.* **11** 041102
- Schmitz C H, Löcker M, Lasker J M, Hielscher A H and Barbour R L 2002 Instrumentation for fast functional optical tomography *Rev. Sci. Instrum.* **73** 429–39
- Taga G, Asakawa K, Maki A, Konishi Y and Koizumi H 2003 Brain imaging in awake infants by near-infrared optical topography *Proc. Natl. Acad. Sci. USA* **100** 10722–27
- Wolf M, Keel M, Dietz V, von Siebenthal K, Bucher H U and Baenziger O 1999 The influence of a clear layer on near-infrared spectrophotometry measurements using a liquid neonatal head phantom *Phys. Med. Biol.* **44** 1743–53
- Yamashita Y, Maki A and Koizumi H 1999 Measurement system for noninvasive dynamic optical topography *J. Biomed. Opt.* **4** 414–7
- Zeff B W, White B R, Dehghani H, Schlaggar B L and Culver J P 2007 Retinotopic mapping of adult human visual cortex with high-density diffuse optical tomography *Proc. Natl. Acad. Sci. USA* **104** 12169–74